NASA TM X-288

TECHNICAL MEMORANDUM

X-288

AN INVESTIGATION AT SUBSONIC SPEEDS OF

AERODYNAMIC CHARACTERISTICS AT ANGLES OF ATTACK FROM

-4° TO 100° OF A DELTA-WING REENTRY CONFIGURATION

HAVING FOLDING WINGTIP PANELS

By Bernard Spencer, Jr.

Langley Research Center
Langley Field, Va.

NATIONAL AERONAUTICS AND SPACE ADMINISTRATION

WASHINGTON May 1960

NATIONAL AERONAUTICS AND SPACE ADMINISTRATION

TECHNICAL MEMORANDUM X-288

AN INVESTIGATION AT SUBSONIC SPEEDS OF AERODYNAMIC CHARACTERISTICS AT ANGLES OF ATTACK FROM -4° TO 100° OF A DELTA-WING REENTRY CONFIGURATION HAVING FOLDING WINGTIP PANELS

By Bernard Spencer, Jr.

SUMMARY

An investigation was made at subsonic speeds in the Langley high-speed 7- by 10-foot tunnel to determine the aerodynamic characteristics of a lifting reentry configuration having folding wingtip panels. The configuration is of the type used in a high angle-of-attack (near 90°) reentry to minimize aerodynamic heating. By unfolding the wingtip panels into the airstream, a moderate angle-of-attack glide is used for a controlled landing. The basic configuration tested utilized a 73° sweptback delta wing and 47.24° sweptback wingtip panels whose area was 25 percent of the total wing area. The effects of varying the plan form and size of the wingtip panels was studied as well as the effects of unfolding the wingtip panels in a high angle-of-attack attitude. Tests were made at Mach numbers of 0.40, 0.60, and 0.80 over an angle-of-attack range from approximately -4° to 100°. A detailed discussion of the results is not presented.

INTRODUCTION

The Langley Research Center of the National Aeronautics and Space Administration is currently conducting a general research program to provide information on the longitudinal and lateral stability and control characteristics associated with several simplified delta-wing configurations considered as possible winged reentry vehicles. The results of some of the previous investigations may be found in references 1 to 7. Reference 4 presents results of a systematic study of the

effect of wing and folding wingtip-panel geometry on the aerodynamic characteristics of possible winged-type reentry vehicles at subsonic speeds. These configurations appear suitable for a high angle-of-attack (near 90°) reentry to minimize the aerodynamic heating and, by unfolding the wingtip panels into the airstream, these configurations are capable of making a controlled landing at normal attitudes. A large range of wing sweep angles was studied and the results indicated that the wing having 73° leading-edge sweep provided the most satisfactory stability characteristics in the glide attitude at subsonic speeds.

The purpose of the present investigation, therefore, was to provide more complete information on the longitudinal stability and control characteristics at subsonic speeds of a 73° sweptback delta wing in a normal flight attitude (i.e., angle-of-attack range from 0° to 50°), and longitudinal and lateral stability and control characteristics of this wing in the reentry attitude (i.e., angle-of-attack range from 60° to 100°). The reentry attitude was included in this subsonic investigation since it may be desirable to delay transition to the glide attitude until subsonic speeds are reached.

SYMBOLS

All data presented in this paper are referenced to the body-axis system except the lift and drag which, of course, are referenced to the wind-axis system. All coefficients are nondimensionalized with respect to the wing-alone (i.e., wingtip panels off) geometric characteristics. The moment-reference location was at the wing-alone centroid of area corresponding to the theoretical wing center-of-pressure location at hypersonic speeds with the vehicle at an angle of attack of 90°.

C_D drag coefficient, $\frac{\text{Drag}}{qS_w}$

C_L lift coefficient, $\frac{\text{Lift}}{qS_w}$

C_l rolling-moment coefficient, $\frac{\text{Rolling moment}}{qS_w b_w}$

C_m pitching-moment coefficient, $\frac{\text{Pitching moment}}{qS_w \bar{c}_w}$

C_n yawing-moment coefficient, $\frac{\text{Yawing moment}}{qS_w b_w}$

C_Y side-force coefficient, $\frac{\text{Side force}}{qS_w}$

b_w wingspan, ft

$\bar{c}_w$ wing mean aerodynamic chord, ft

i_t wingtip-panel incidence angle, deg

M Mach number

q dynamic pressure, lb/sq ft

S_w wing area, sq ft

α angle of attack, deg

δ_f wing trailing-edge flap deflection, deg

δ_h wingtip-panel deflection from position perpendicular to wing chord plane (fig. 1(a)), deg

ϕ angle of roll, deg

Subscripts:

L left wingtip panel

R right wingtip panel

Model component designations:

W basic 73° sweptback delta wing (without wingtip panels and trailing-edge flap)

H_0 47.24° sweptback wingtip panel having area of $0.25S_w$

H_1 unswept wingtip panel having area of $0.364S_w$

H_2 unswept wingtip panel having area of $0.25S_w$

MODELS, TESTS, AND CORRECTIONS

The basic delta wing used in this investigation had a leading-edge sweep angle of 73° and was of flat-plate section with a rounded leading edge and a blunt trailing edge. (See fig. 1(a).) The wingtip panels were of similar cross section, except for beveled trailing edges. Wingtip-panel deflections have been measured from the condition of panel chord plane perpendicular to the wing chord plane. Therefore, positive deflections of the wingtip panels occur as the panels are unfolded into the airstream. One wingtip panel H_0 had a leading-edge sweep of 47.24° and a total area of $0.25S_w$. The unswept panel H_1 had a span equal to that of the swept panel H_0 and an area of $0.364S_w$. Wingtip panel H_2 was also unswept and had a total area equal to that for panel H_0 ($0.25S_w$). These panels could be displaced vertically 1.25 inches by means of fins located at the wingtip. (See fig. 1(b).)

A full-span trailing-edge flap with a beveled trailing edge was used on the basic delta wing. The total flap area was $0.08S_w$, and the plan form is shown in figure 1(b). No vertical tails were employed in the investigation other than fins employed for wingtip-panel displacement.

Tests were made in the Langley high-speed 7- by 10-foot tunnel for a Mach number range from 0.40 to 0.80 corresponding to a Reynolds number range from approximately 2.6×10^6 to 4.6×10^6 based on the wing-alone mean aerodynamic chord. The model was tested through an angle-of-attack range from -4° to 100° for Mach numbers of 0.40, 0.60, and 0.80 and a roll-angle range from -10° to 10° at an angle of attack of 90° for Mach numbers of 0.40 and 0.60. The sting-support arrangements of a similar model for the low angle-of-attack tests and the high angle-of-attack tests are shown in figure 2. Jet-boundary corrections determined by the methods of reference 8 and blockage corrections determined by the methods of reference 9 were found to be negligible because of the small size of the model and, therefore, were not applied to the data. The angle of attack has been corrected for deflection of the sting-support system under load.

RESULTS

In this section the results are briefly outlined and only a few pertinent observations are made.

The effects of wingtip-panel deflection on the longitudinal stability characteristics of the basic delta-wing model WH_0 in the high-angle

reentry attitude are presented in figure 3. Tests were begun with the model at 100° angle of attack to simulate the attitude of the actual configuration in transition from the reentry to the glide flight condition. Of particular interest is the fact that a pitching-moment reversal occurs between $\delta_h = 30°$ and $\delta_h = 50°$. Initially a small positive pitching moment is produced between $\delta_h = 0°$ and $\delta_h = 30°$ and results in a trim condition above an angle of attack of 90°, which renders small negative lift-drag ratios. This pitching-moment reversal is apparently due to a pressure recovery, which for these moderate deflections offsets the increase in frontal area. These folding-type wingtip panels are not contemplated to be used as control devices in the high angle-of-attack region but rather would unfold at a programed rate to initiate transition to a glide flight position. Other controls located at the wing apex or small tabs located at the wingtips would be available to offset any initial reversals in pitching moment.

However, if the center of gravity of the vehicle were located so that it was trimmed at 90° angle of attack and 0° wingtip-panel deflection, a situation would exist in which unfolding the wingtip panels up to 30° would result in small negative lift-drag ratios. This could be of importance in connection with trajectory control.

Figure 4 presents the effects of differential deflection of the wingtip panels on the lateral stability characteristics of the basic delta-wing model WH_0 at 90° angle of attack.

The effects of the swept wingtip panel on the longitudinal stability characteristics of the 73° delta-wing configuration in a normal flight attitude are presented in figure 5, and the results are quite similar to those presented in reference 4. Tests were begun with the model at an angle of attack of approximately -4° for all normal-attitude tests. An interesting point to note is the pronounced effect of the wingtip panels in linearizing and increasing the lift-curve slope. A discussion of this effect may be found in reference 4.

The effectiveness in providing longitudinal control to the delta-wing model WH_0 by deflection of a wing trailing-edge flap is presented in figure 6. Figure 7 presents the effects on the longitudinal stability and control characteristics of the delta-wing model WH_0 of displacing the swept wingtip panel H_0 vertically as well as those for the swept wingtip panel in the chord plane of the wing. The results are quite similar to those obtained on the basic configuration of reference 4 in that the vertical displacement of the swept wingtip panel H_0 reduced the lift considerably and caused an earlier reversal in slope of pitching-moment variation with angle of attack.

Wingtip-panel plan-form effects on the longitudinal stability characteristics of the delta-wing model WH_0 are presented in figure 8. Figure 9 indicates the effects of hysteresis associated with the basic delta-wing model WH_0 in an angle-of-attack range from -4° to 87° and at Mach numbers of 0.40 and 0.60. These results were obtained by starting the tests with the configuration at $\alpha \approx 87^\circ$; a comparison with tests begun at $\alpha = 0^\circ$ is included. The largest effects are noted in the region of stall, as would be expected.

Langley Research Center,
National Aeronautics and Space Administration,
Langley Field, Va., February 23, 1960.

REFERENCES

1. Paulson, John W.: Low-Speed Static Stability Characteristics of Two Configurations Suitable for Lifting Reentry From Satellite Orbit. NASA MEMO 10-22-58L, 1958.

2. Paulson, John W., and Shanks, Robert E.: Investigation of Low-Subsonic Flight Characteristics of a Model of a Flat-Bottom Hypersonic Boost-Glide Configuration Having a 78° Delta Wing. NASA TM X-201, 1959.

3. Petynia, William W.: Model Investigation of Water Landings of a Winged Reentry Configuration Having Outboard Folding Wing Panels. NASA TM X-62, 1959.

4. Spencer, Bernard, Jr.: High-Subsonic-Speed Investigation of the Static Longitudinal Aerodynamic Characteristics of Several Delta-Wing Configurations for Angles of Attack From 0° to 90°. NASA TM X-168, 1959.

5. Foster, Gerald V.: Exploratory Investigation at Mach Number of 2.01 of the Longitudinal Stability and Control Characteristics of a Winged Reentry Configuration. NASA TM X-178, 1959.

6. Fournier, Paul G.: Wind-Tunnel Investigation at High Subsonic Speed of the Static Longitudinal Stability Characteristics of a Winged Reentry Vehicle Having a Large Negatively Deflected Flap-Type Control Surface. NASA TM X-179, 1959.

7. Ware, George M.: Low-Subsonic-Speed Static Longitudinal Stability and Control Characteristics of a Winged Reentry-Vehicle Configuration Having Wingtip Panels That Fold Up for High-Drag Reentry. NASA TM X-227, 1960.

8. Gillis, Clarence L., Polhamus, Edward C., and Gray, Joseph L., Jr.: Charts for Determining Jet-Boundary Corrections for Complete Models in 7- by 10-Foot Closed Rectangular Wind Tunnels. NACA WR L-123, 1945. (Formerly NACA ARR L5G31.)

9. Herriot, John G.: Blockage Corrections for Three-Dimensional-Flow Closed-Throat Wind Tunnels, With Consideration of the Effect of Compressibility. NACA Rep. 995, 1950. (Supersedes NACA RM A7B28.)

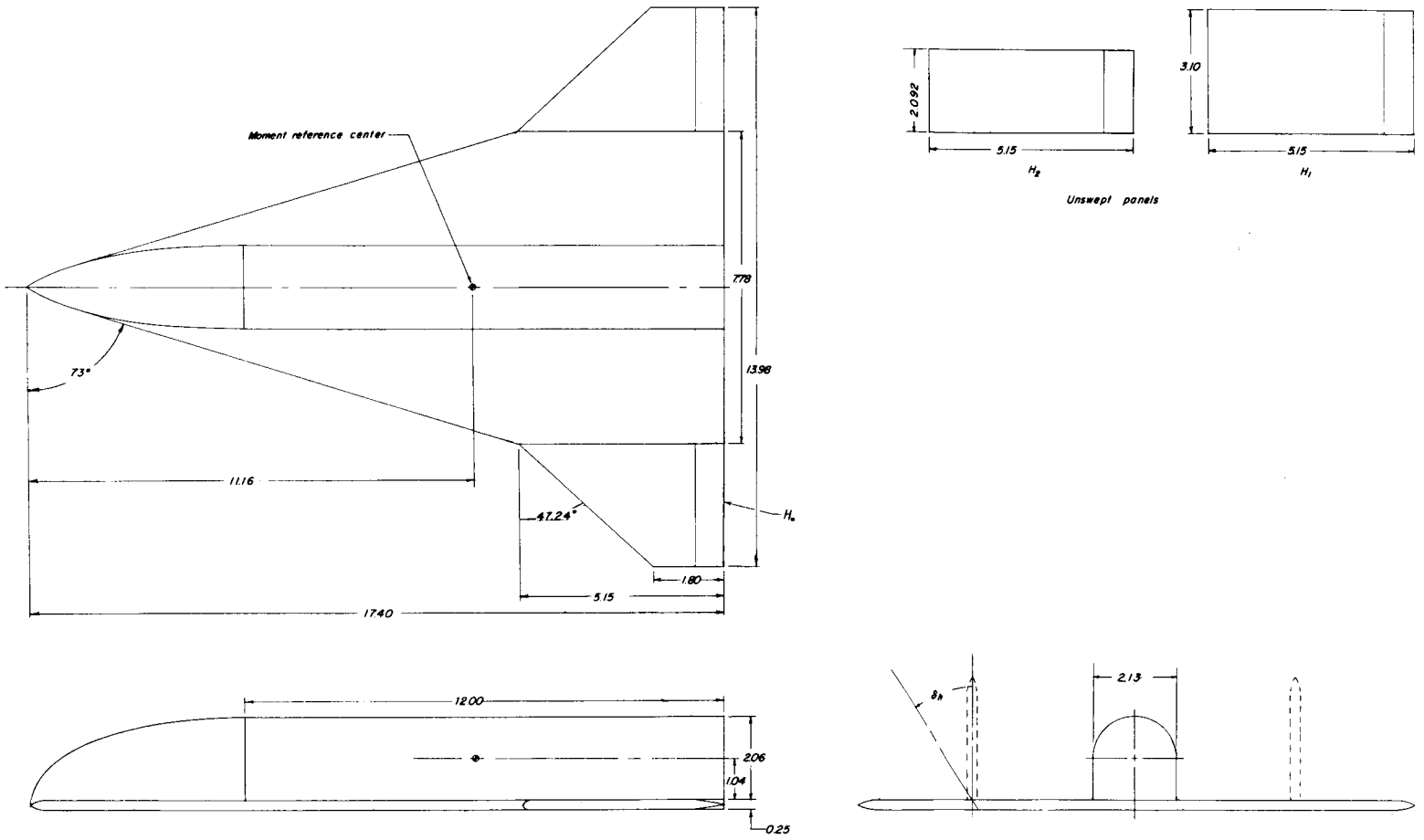

(a) Basic delta-wing and swept wingtip panel, and details of unswept wingtip panels.

Figure 1.- Geometric characteristics of models used in this investigation. All dimensions are in inches.

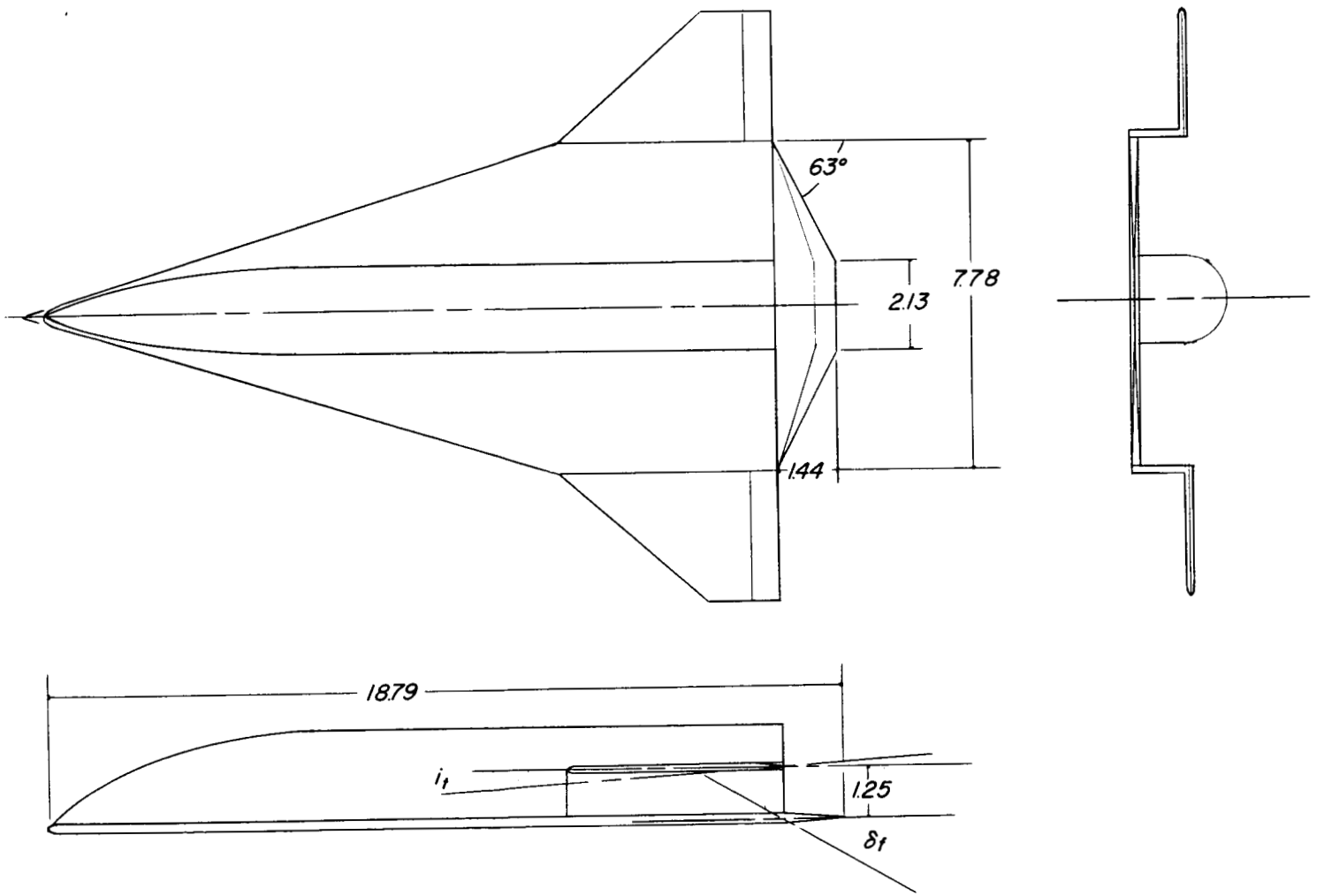

(b) Revisions to basic plan form including wing trailing-edge flap and displaced wingtip panel.

Figure 1.- Concluded.

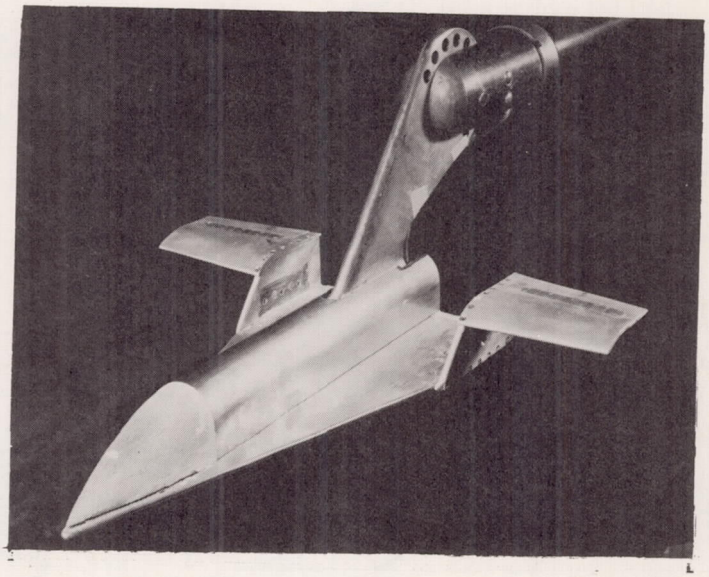

L-59-3159

(a) Mounting strut in normal attitude for tests at low angles of attack.

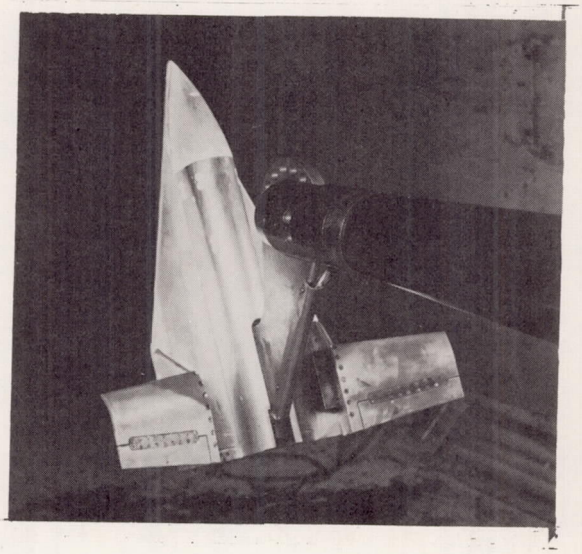

L-59-3162

(b) Mounting strut reversed for tests at high angles of attack.

Figure 2.- Model mounting arrangement for high-angle attitude and normal attitude. The configuration shown in the photograph is similar to the one used in the present investigation.

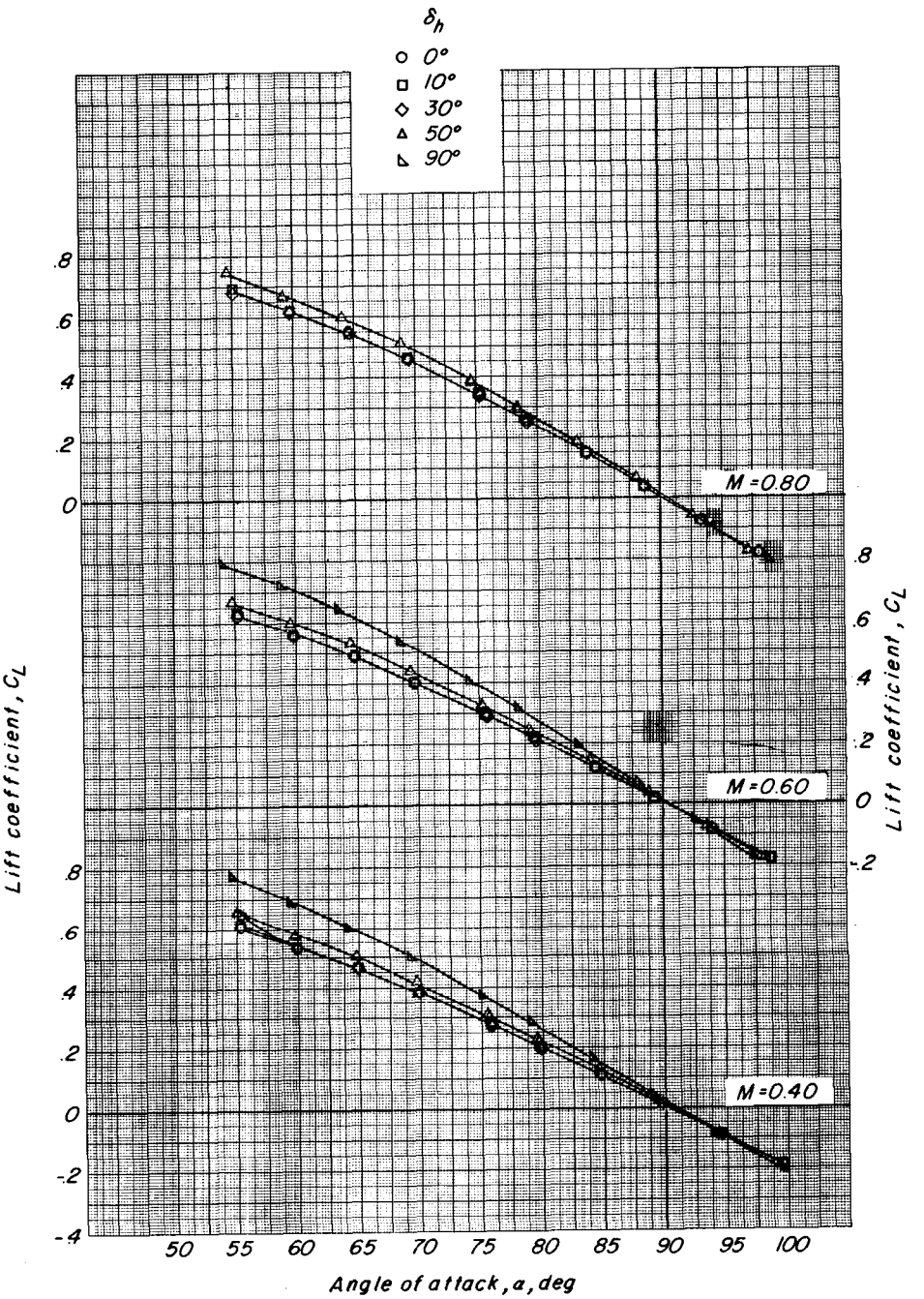

(a) Variation of lift coefficient with angle of attack.

Figure. 3.- The effects of deflecting the swept wingtip panels H_0 on the longitudinal stability characteristics of the 73° sweptback wing at high angles of attack.

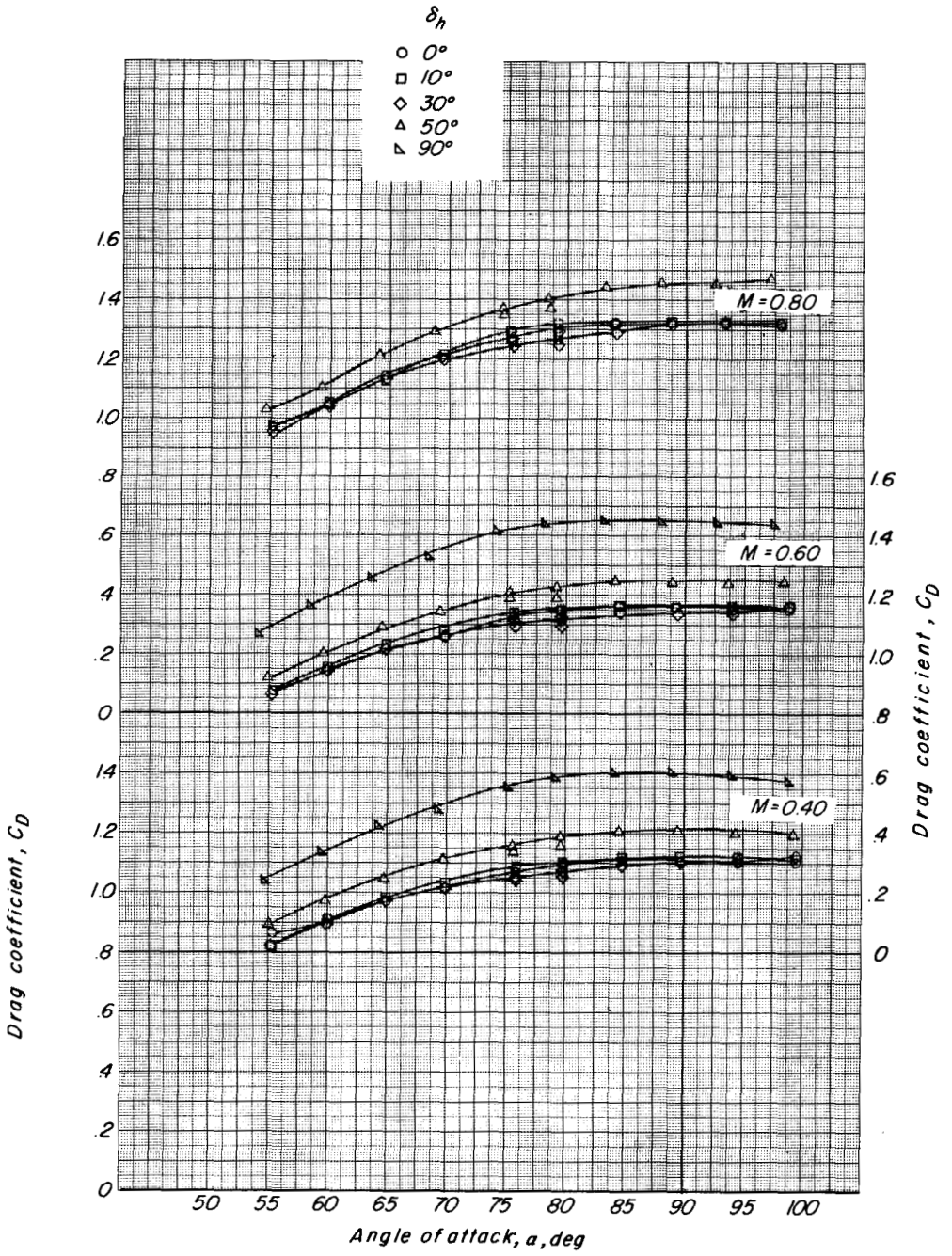

(b) Variation of drag coefficient with angle of attack.

Figure 3.- Continued.

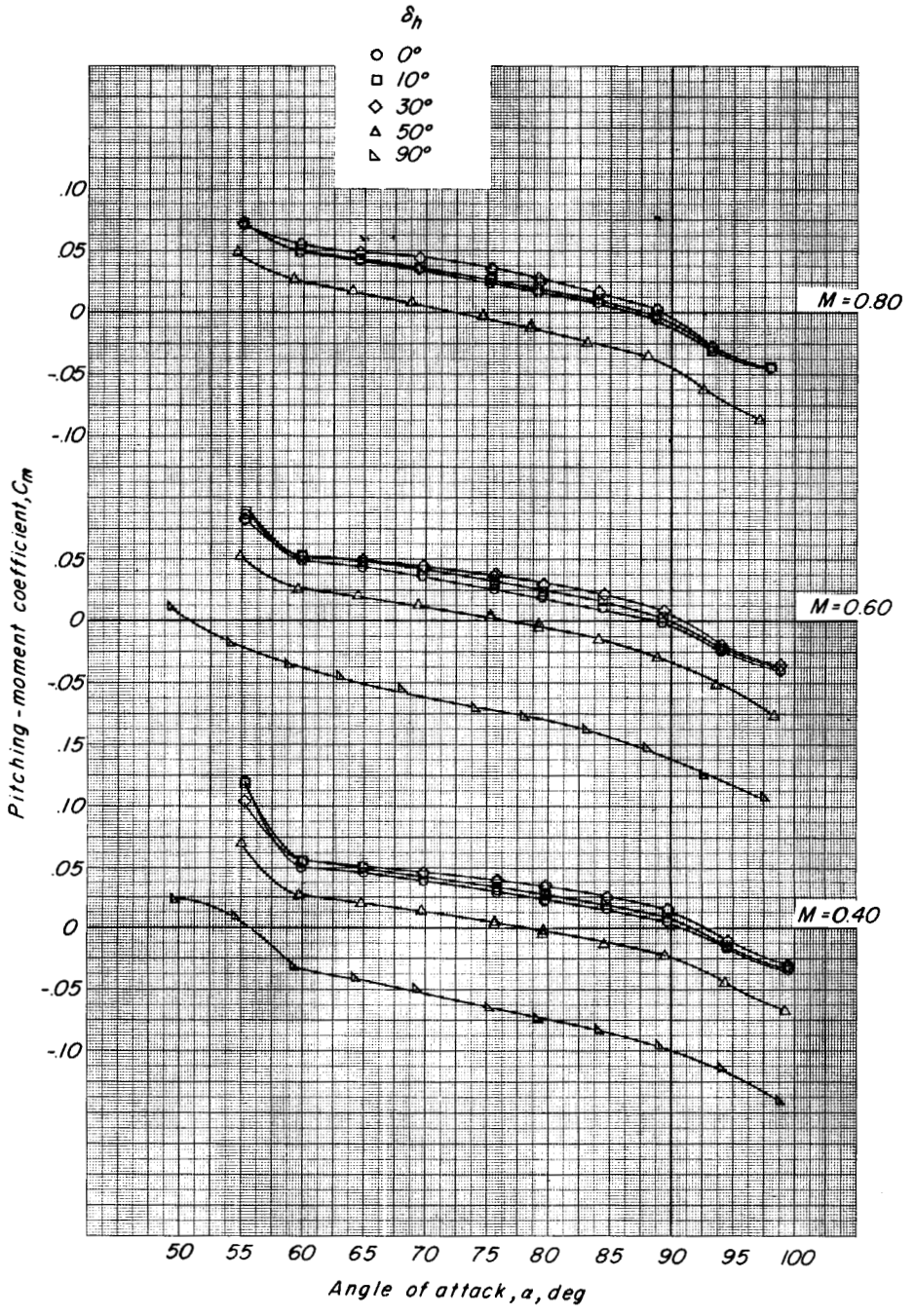

(c) Variation of pitching-moment coefficient with angle of attack.

Figure 3.- Concluded.

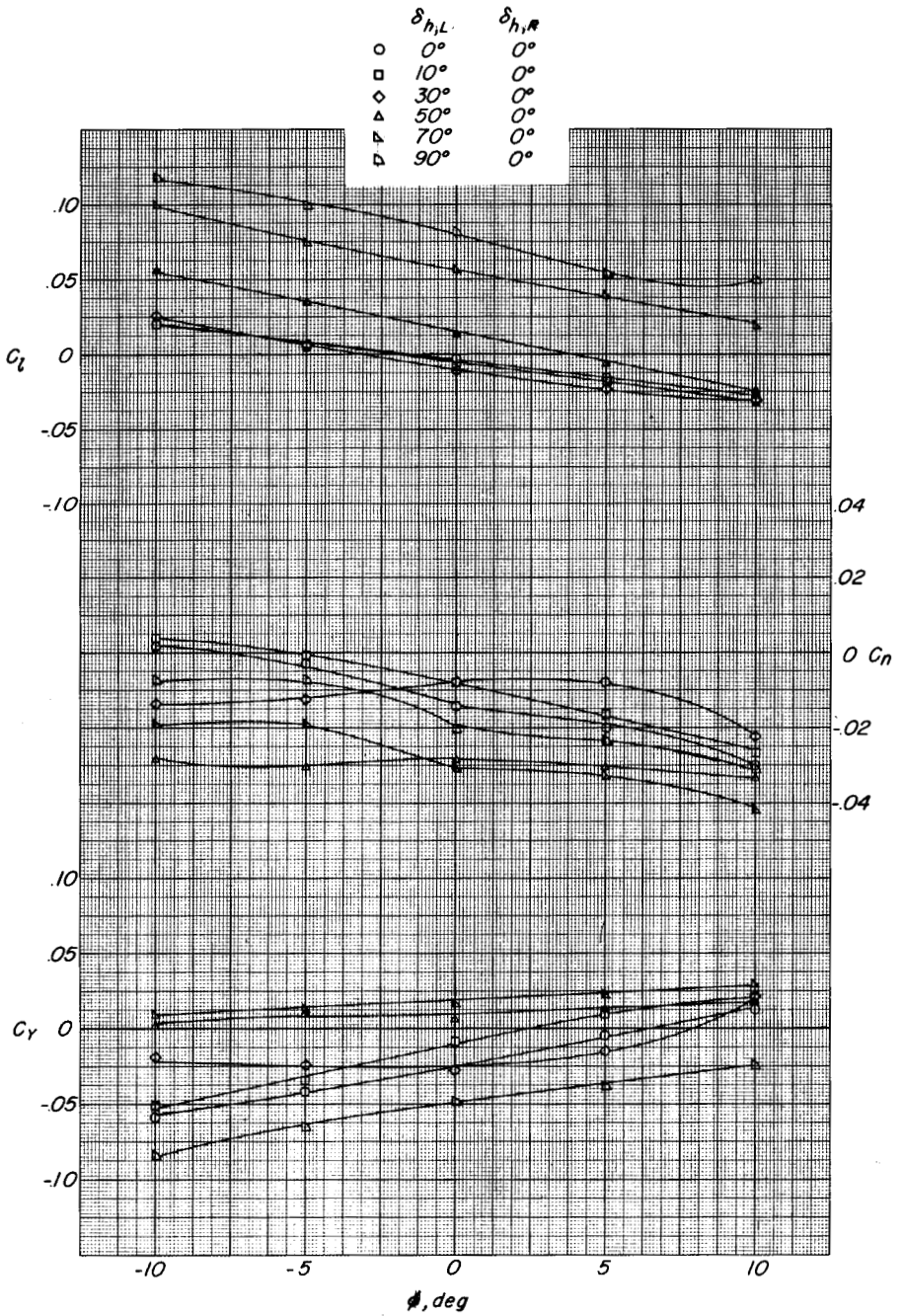

(a) M = 0.40.

Figure 4.- The effects of differential deflection of the wingtip panels on the lateral stability characteristics of the basic delta-wing configuration WH_0 at an angle of attack of 90°.

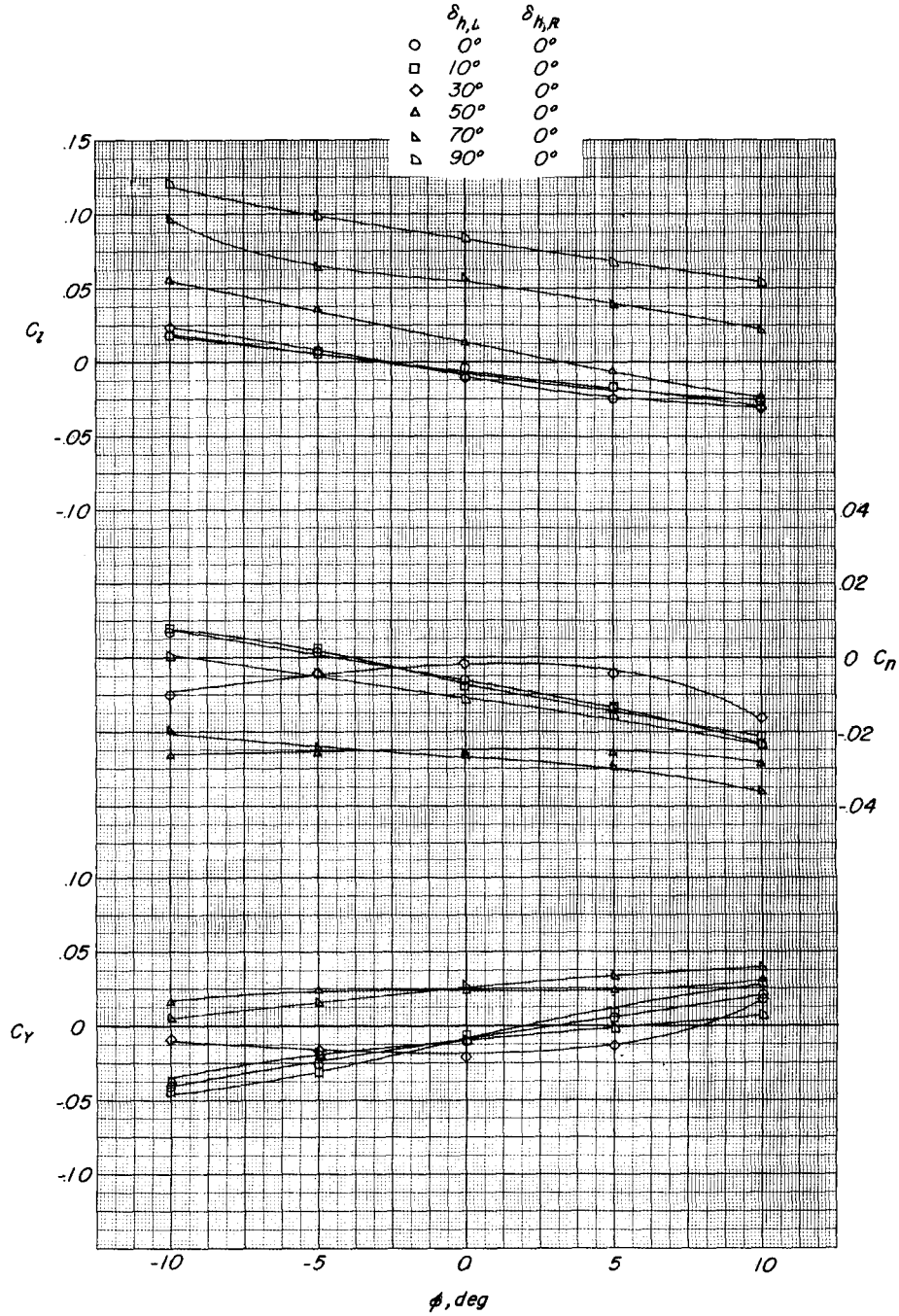

(b) M = 0.60.

Figure 4.- Concluded.

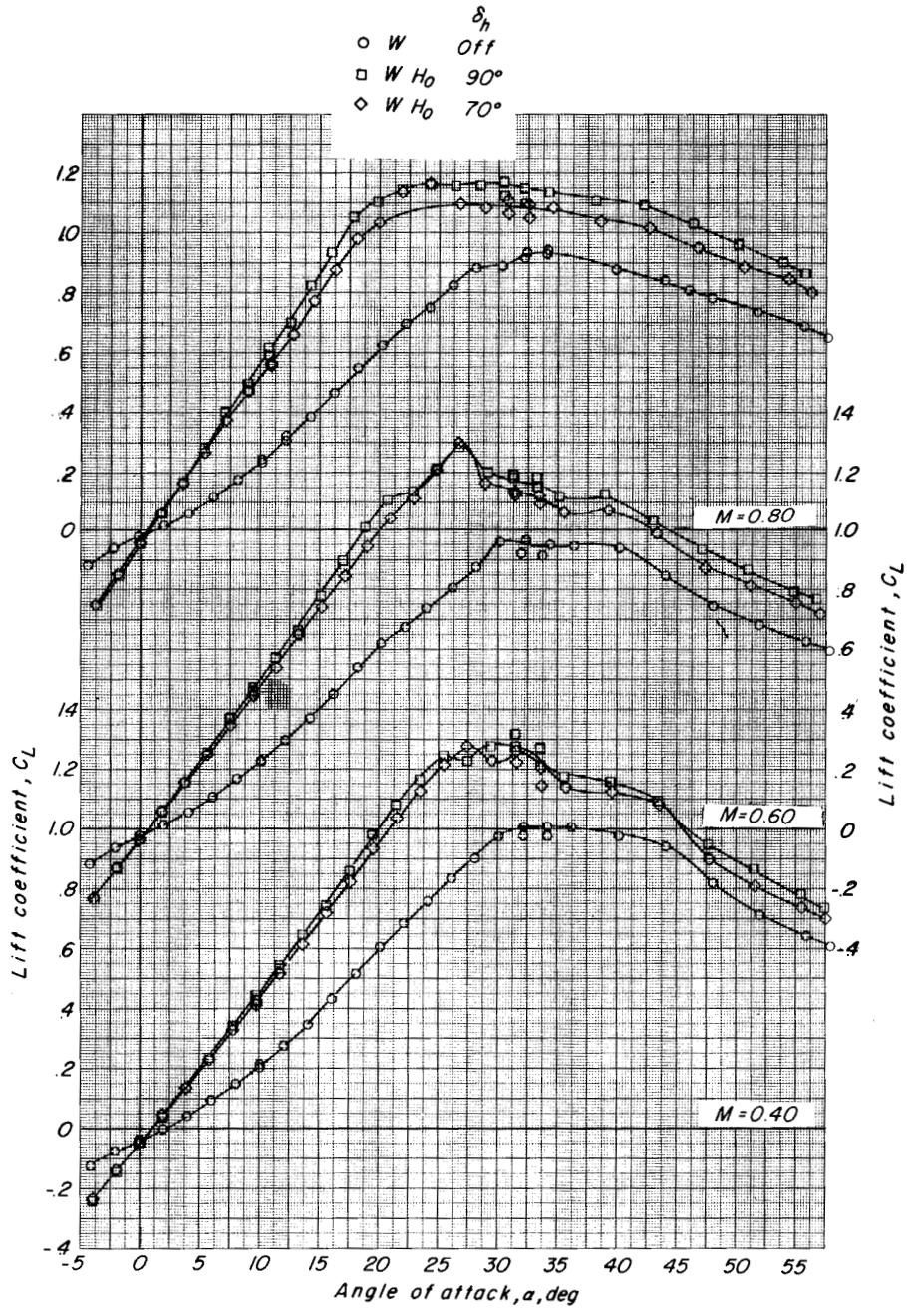

(a) Variation of lift coefficient with angle of attack.

Figure 5.- The effects of the addition and deflection of the swept wing-tip panels H_0 on the longitudinal stability characteristics of the 73° sweptback wing in a normal attitude.

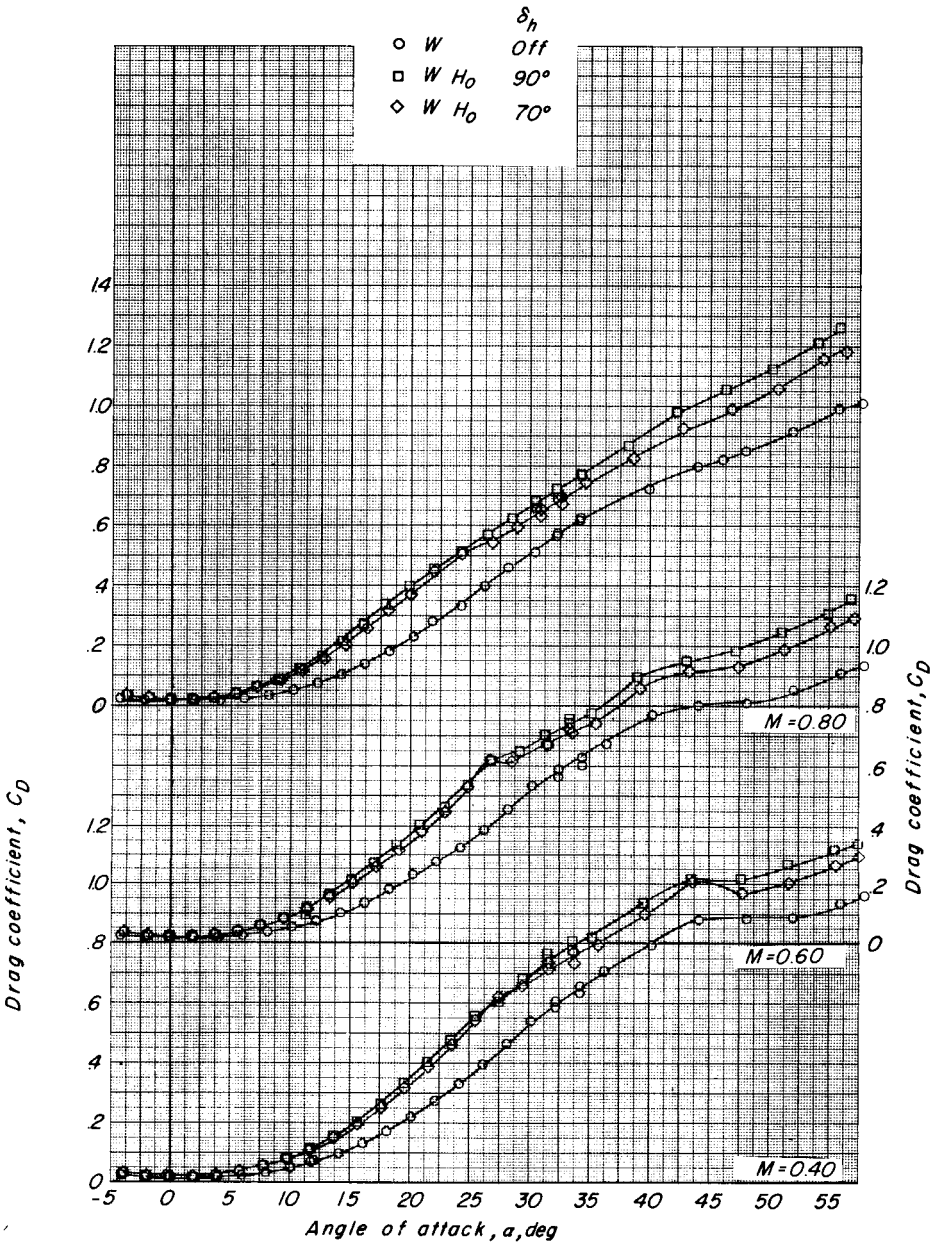

(b) Variation of drag coefficient with angle of attack.

Figure 5.- Continued.

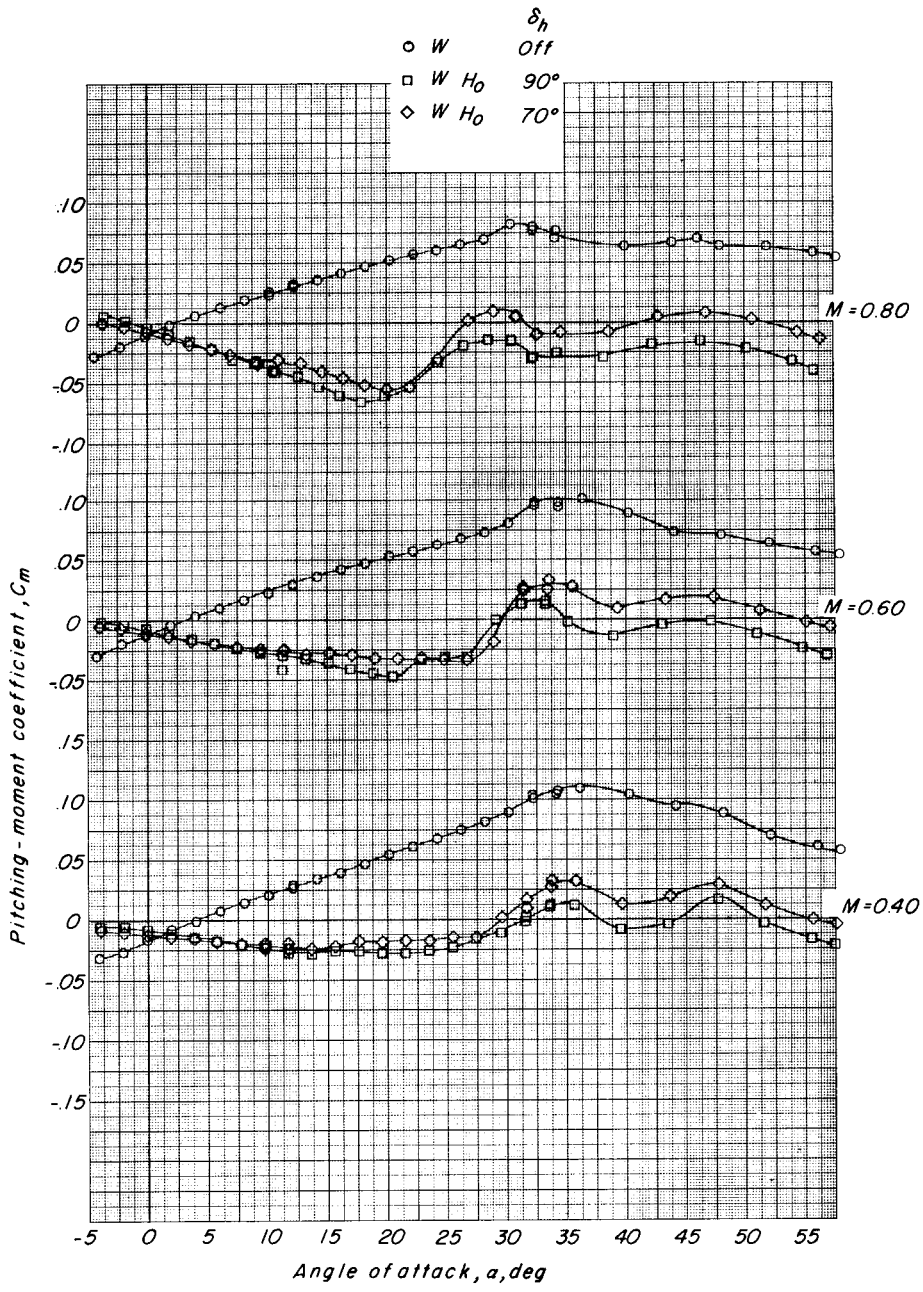

(c) Variation of pitching-moment coefficient with angle of attack.

Figure 5.- Concluded.

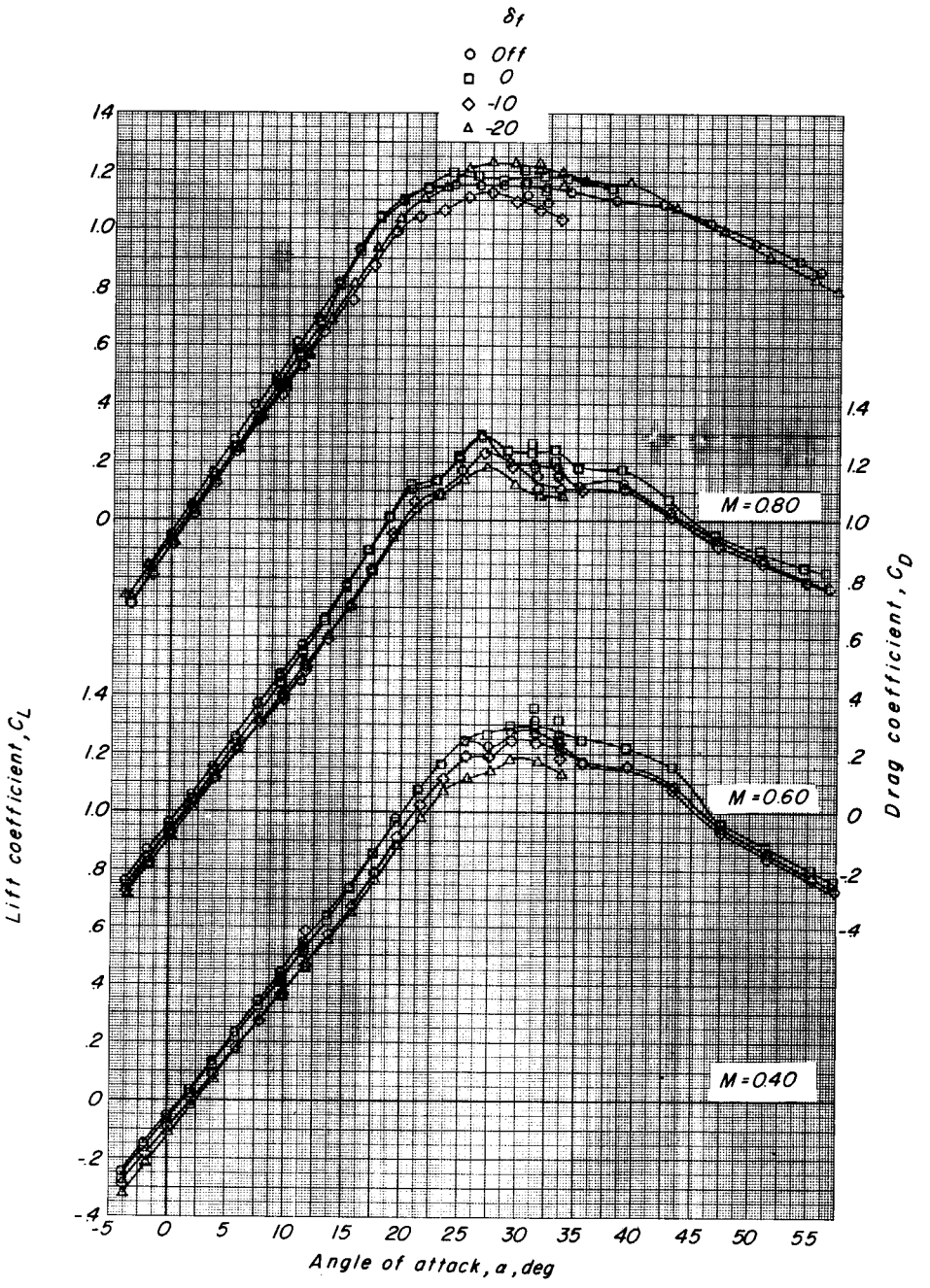

(a) Variation of lift coefficient with angle of attack.

Figure 6.- The effects of the addition and deflection of a wing trailing-edge flap on the longitudinal control characteristics of the 73° sweptback wing with swept wingtip panels H_0. $\delta_h = 90°$.

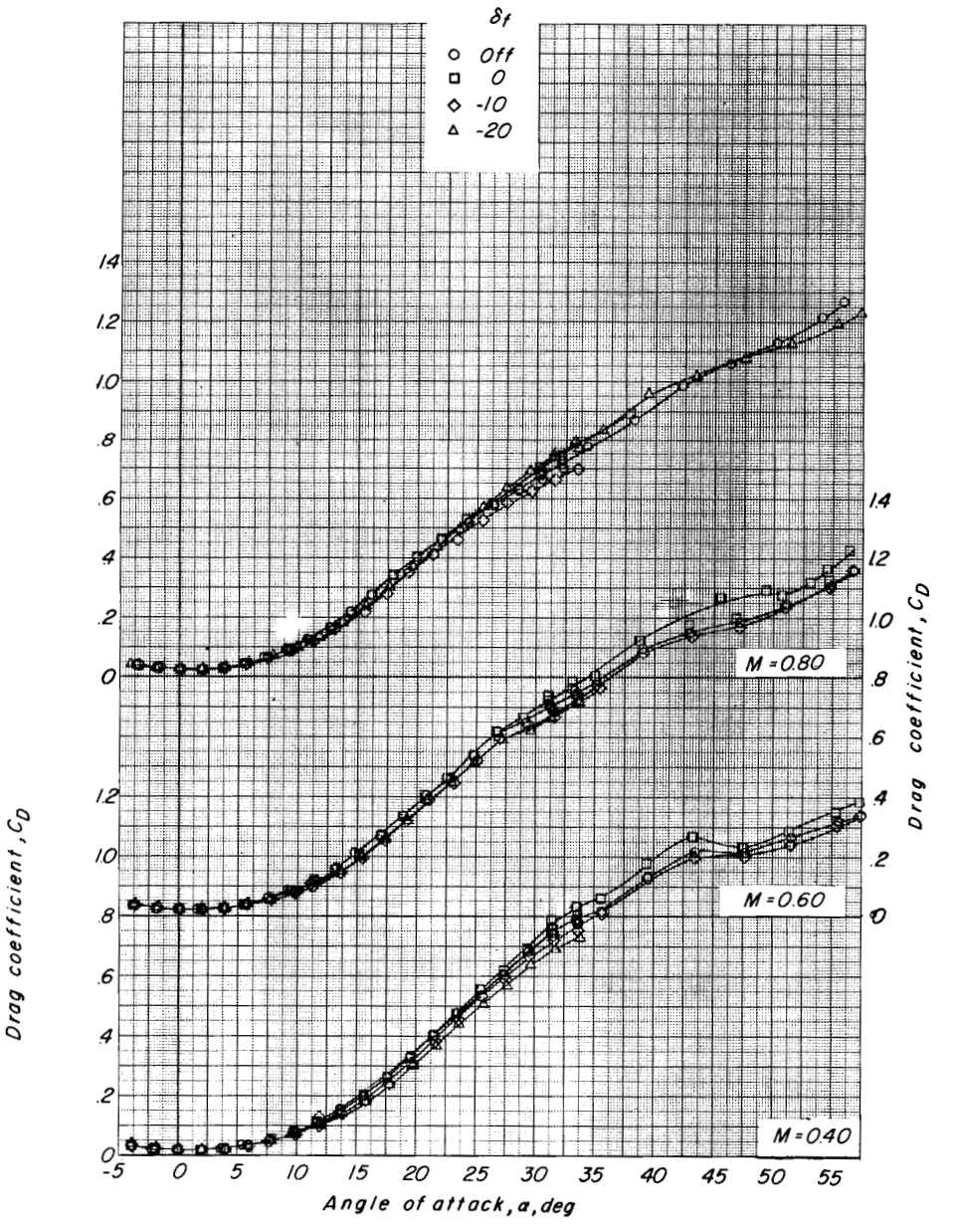

(b) Variation of drag coefficient with angle of attack.

Figure 6.- Continued.

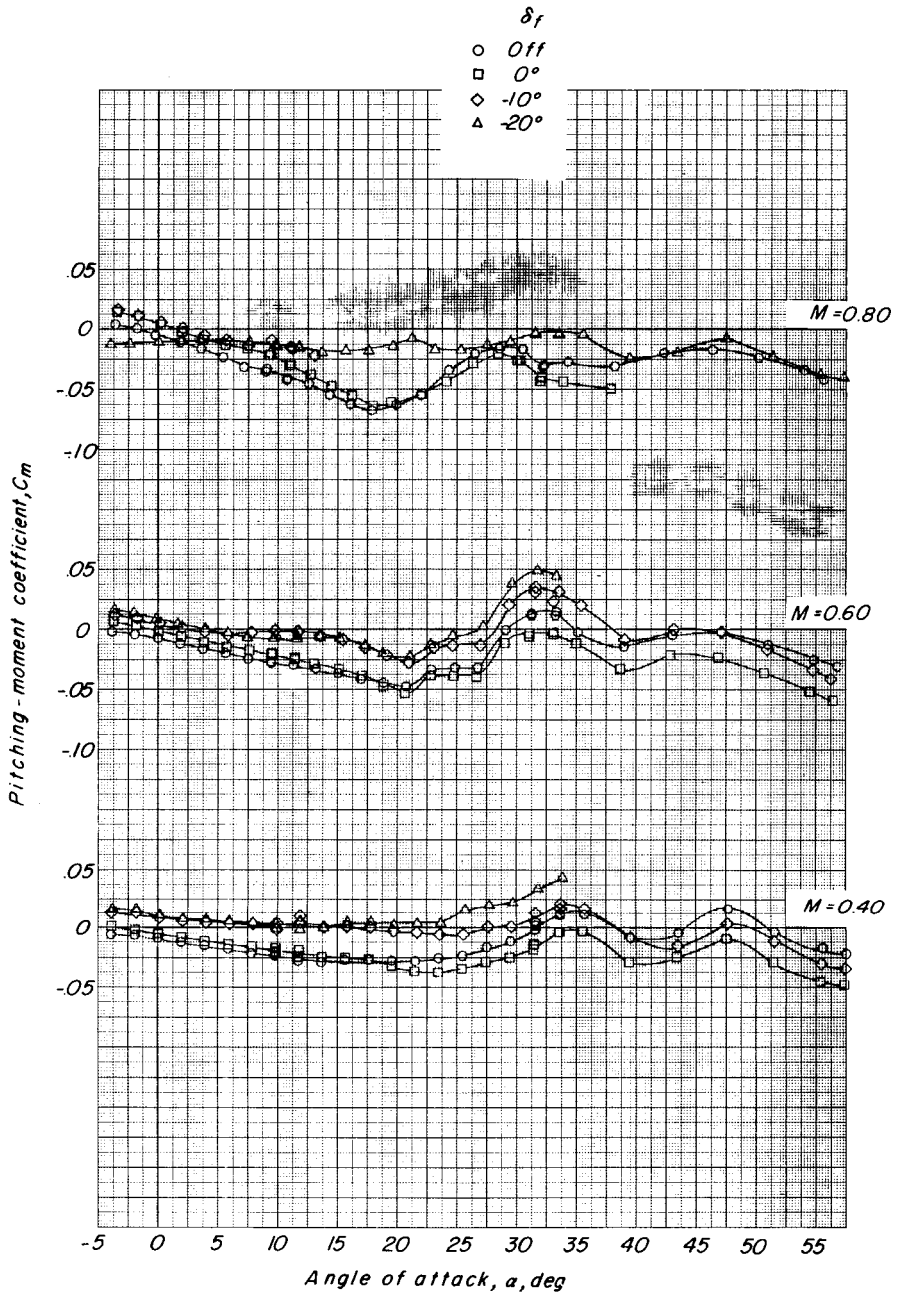

(c) Variation of pitching-moment coefficient with angle of attack.

Figure 6.- Concluded.

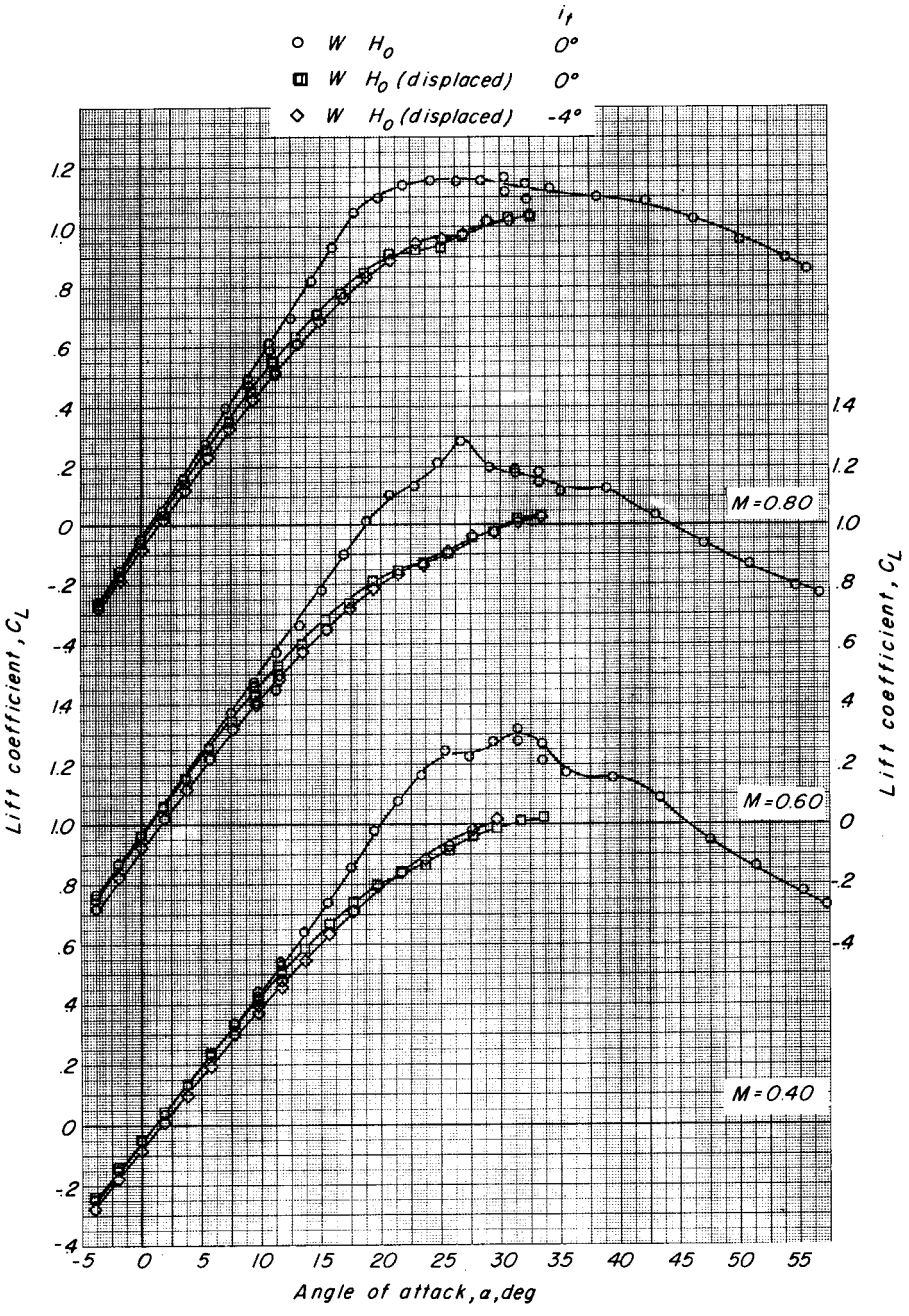

(a) Variation of lift coefficient with angle of attack.

Figure 7.- The effects of displacement and incidence of the swept wingtip panel H_0 on the longitudinal stability and control characteristics of the 73° sweptback wing. $\delta_h = 90°$.

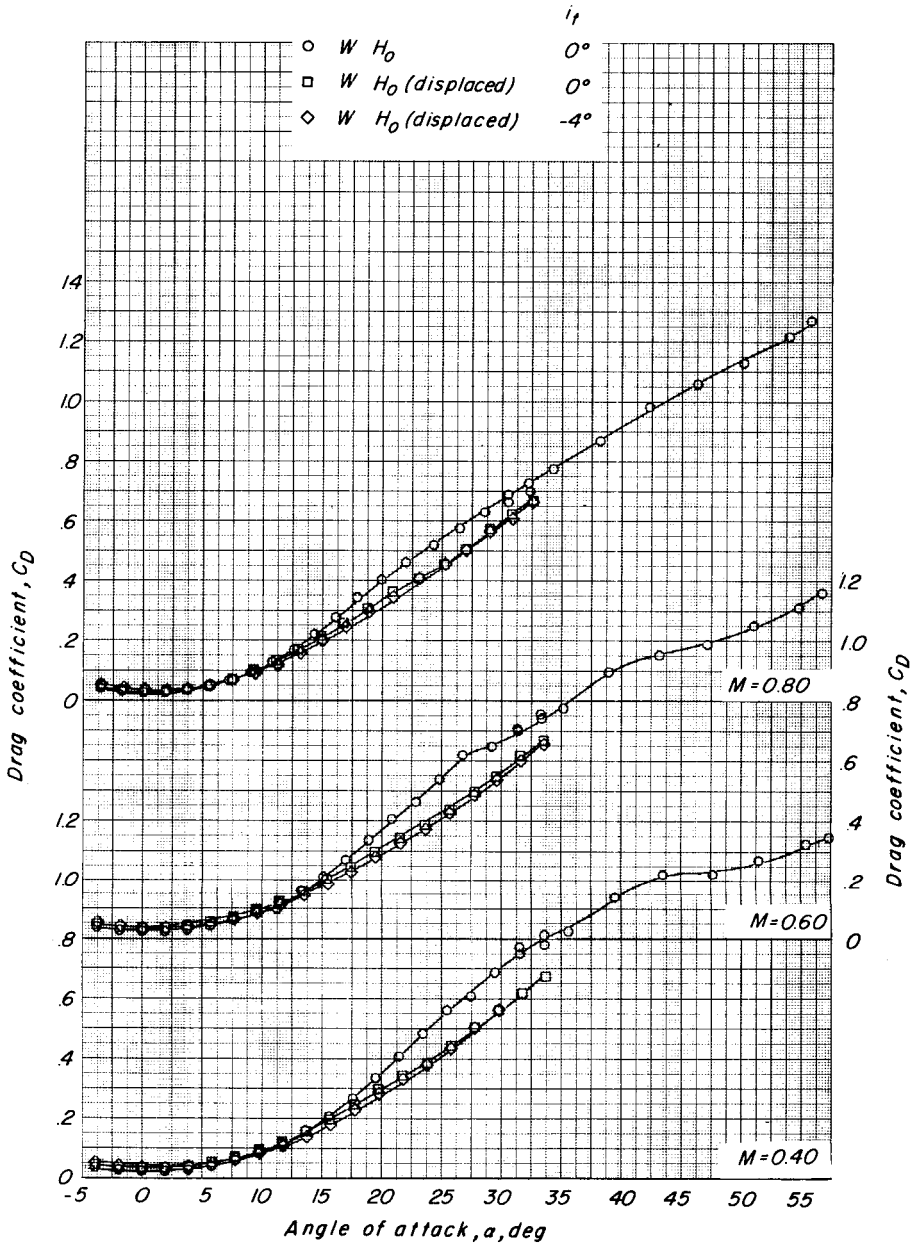

(b) Variation of drag coefficient with angle of attack.

Figure 7.- Continued.

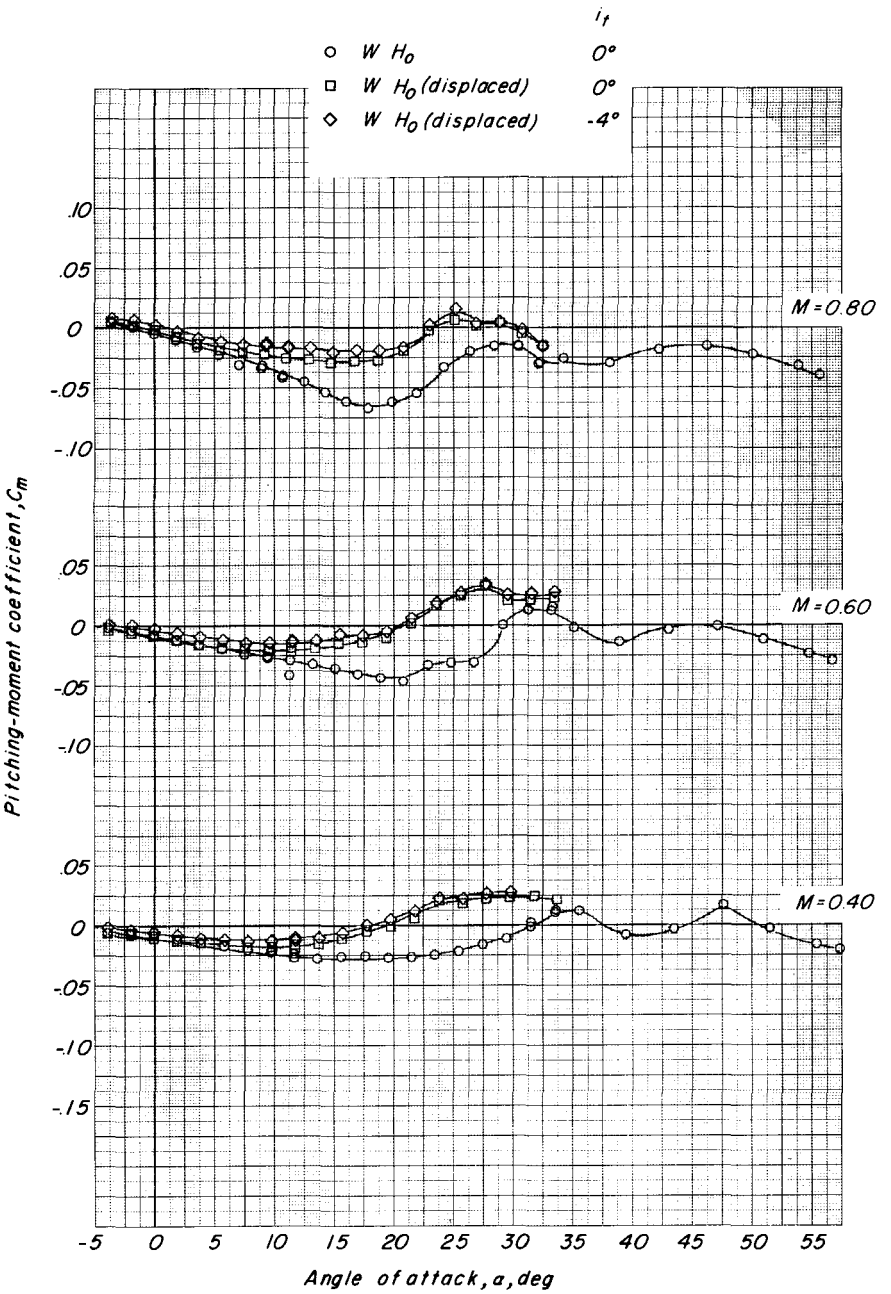

(c) Variation of pitching-moment coefficient with angle of attack.

Figure 7.- Concluded.

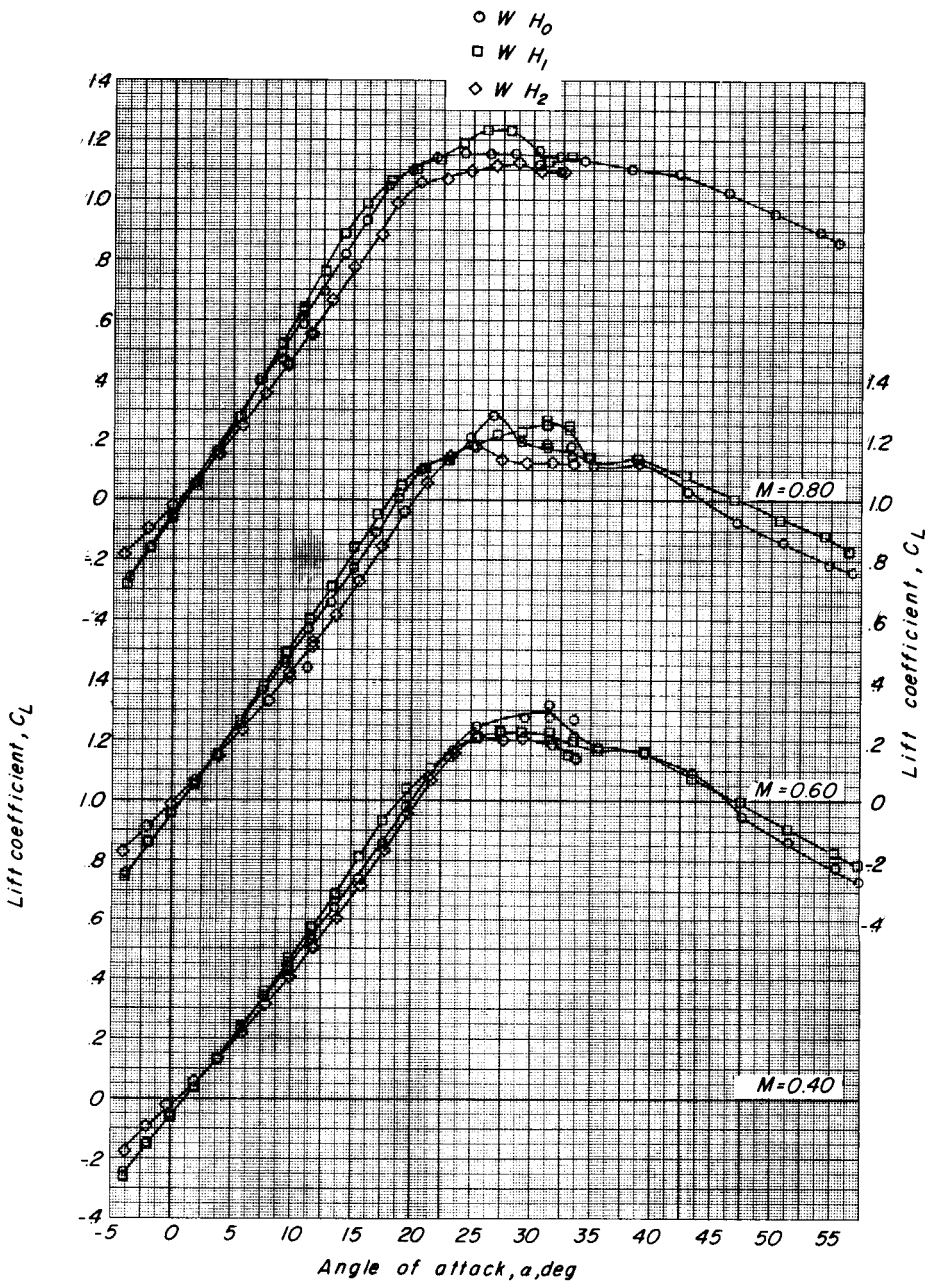

(a) Variation of lift coefficient with angle of attack.

Figure 8.- A comparison of the effects of wingtip-panel plan-form and size variations on the longitudinal stability characteristics of the 73° sweptback wing. $\delta_h = 90°$.

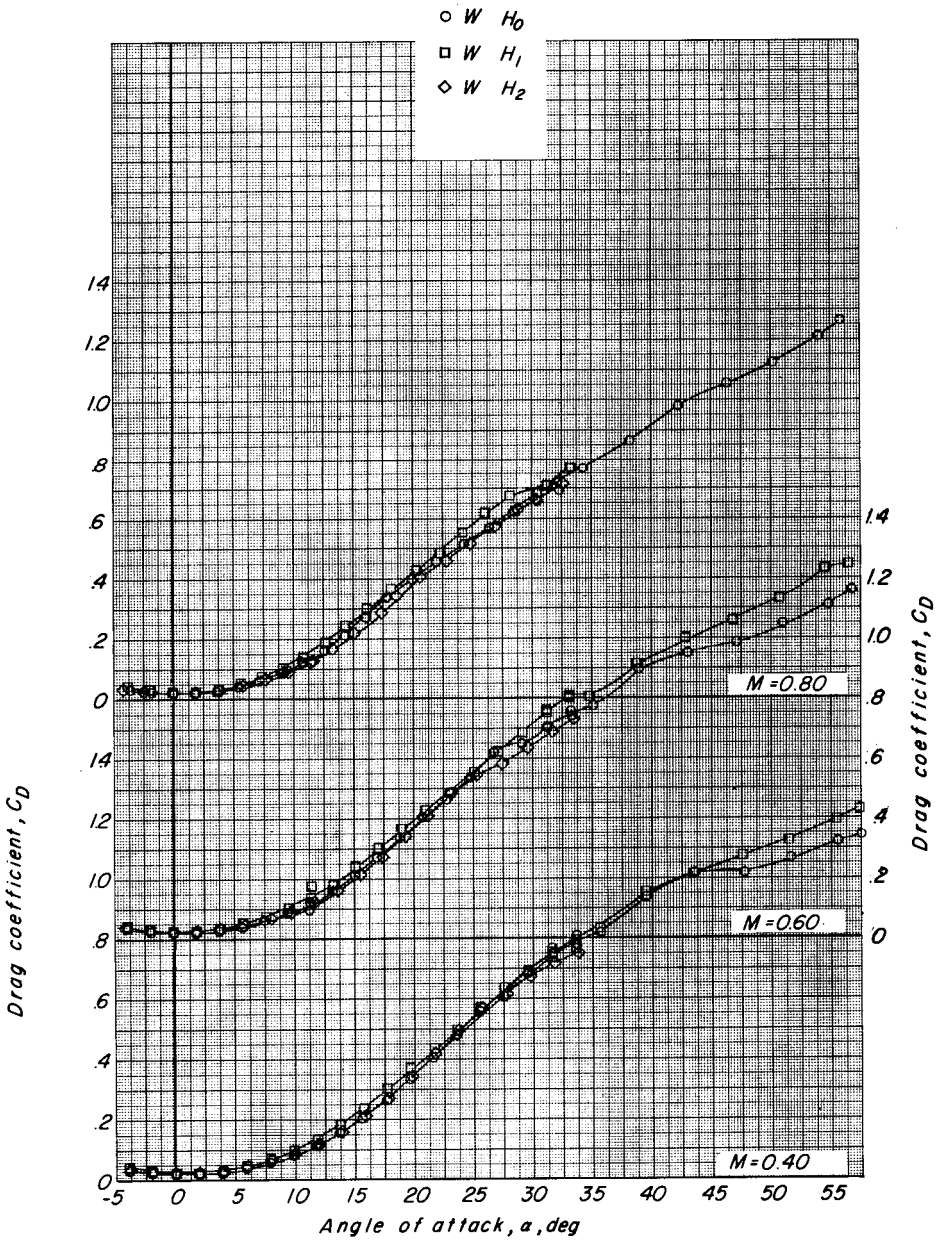

(b) Variation of drag coefficient with angle of attack.

Figure 8.- Continued.

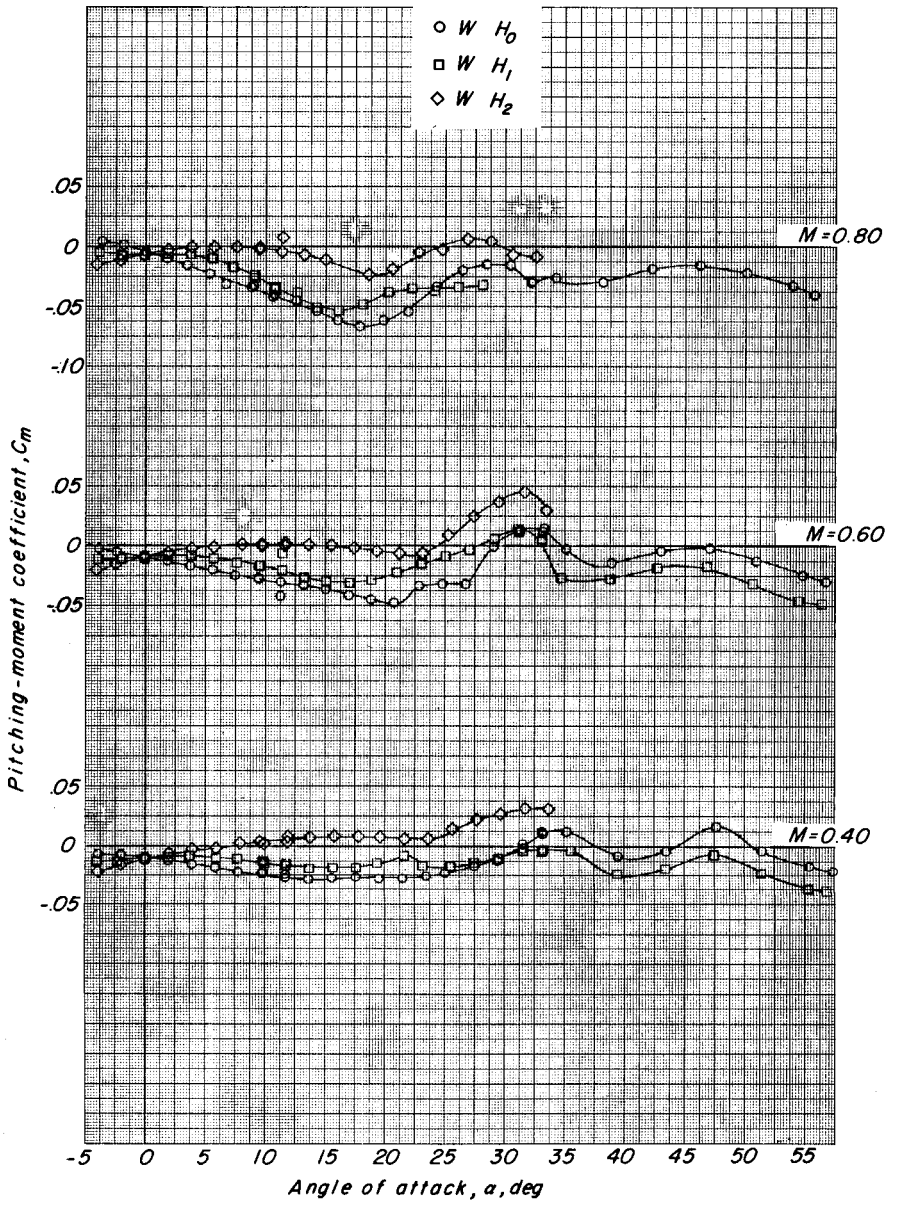

(c) Variation of pitching-moment coefficient with angle of attack.

Figure 8.- Concluded.

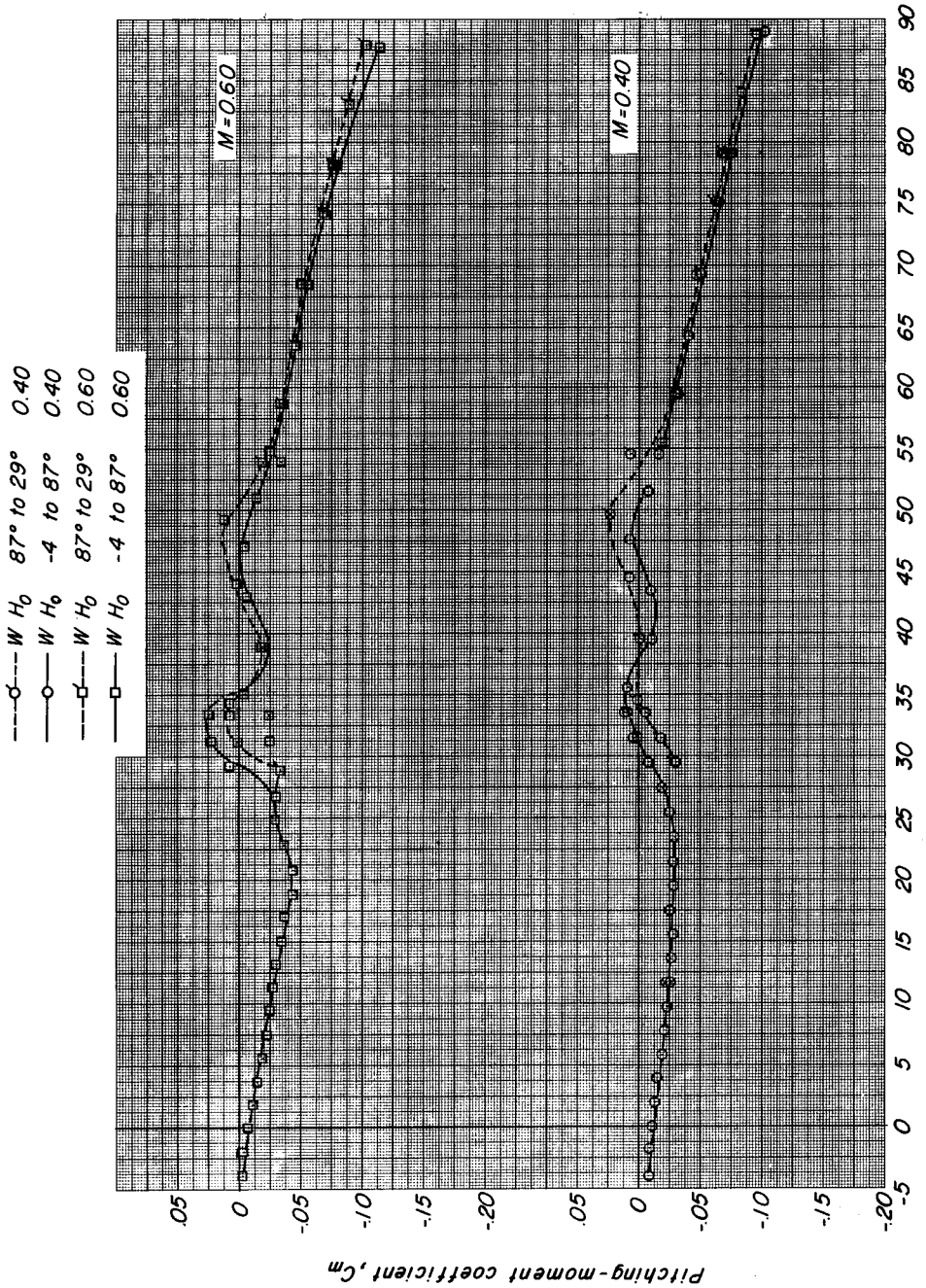

Figure 9.- The effects of hysteresis in the region of stall on the 73° sweptback wing with swept wingtip panels H_O. Dashed lines and flagged symbols indicate angle-of-attack test beginning at approximately 87°. $\delta_h = 90°$.